

Polymeric Foaming Predictions from the Sanchez-Lacombe Equation of State: Application to Polypropylene-Carbon Dioxide Mixtures

Kier von Konigslow,¹ Chul B. Park,² and Russell B. Thompson^{1,*}

¹*Department of Physics and Astronomy and Waterloo Institute for Nanotechnology, University of Waterloo, 200 University Avenue West, Waterloo, Ontario N2L 3G1, Canada*

²*Department of Mechanical and Industrial Engineering, University of Toronto, 5 King's College Road, Toronto, Ontario M5S 3G8, Canada*

(Received 1 May 2017; published 19 October 2017)

A simple off-lattice method of deriving the Sanchez-Lacombe equation of state is presented. The Sanchez-Lacombe equation of state for mixtures is shown to be thermodynamically inconsistent for all mixing rules in such a way that fugacity coefficients, until now thought to correct for mixing inconsistencies, cannot make the theory consistent. The theory is consistent, however, for constant hole volumes and it is shown, for a sample mixture of polypropylene and carbon dioxide, that excellent agreement with experimental solubility results is achieved without changing the mixture parameters with temperature or pressure. To this end, pure-component Sanchez-Lacombe characteristic parameters for both branched and linear polypropylene are also provided. The agreement between theory and experiment for solubility using a constant hole volume for carbon dioxide mixtures with both branched and linear polypropylene is much better than for typical mixing rules for the Sanchez-Lacombe equation of state. Fair agreement with experimental swelling-ratio data at saturation is also achieved with no further free parameters, making this equation of state a good choice for predictions related to polymeric foaming. A consideration of the hole volume is given in terms of correlations, and evidence to support this perspective is presented in terms of the characteristic parameters regressed from different architectures of pure polypropylene. It is shown that only a single pure-polypropylene characteristic parameter is needed to characterize mixtures with carbon dioxide, and that an estimate of this parameter can be extracted from mixture solubility data. This example demonstrates the feasibility of applying the Sanchez-Lacombe equation of state to mixtures in which one of the pure components has not been independently characterized.

DOI: [10.1103/PhysRevApplied.8.044009](https://doi.org/10.1103/PhysRevApplied.8.044009)

I. INTRODUCTION

Polymeric foams are used in a wide range of applications, ranging from packaging, insulation, construction, automotive and aircraft components, sports equipment, medical applications, to other areas [1]. These foams, which consist of gaseous voids surrounded by a denser polymer, can take on structures as diverse as the applications. One key to controlling the cell structure of foams is the interaction between the polymer and the blowing agent which, in the case of physical blowing agents, creates the voids through a thermodynamic instability caused either by a rapid pressure drop or a temperature increase. Clearly, the pressure-volume-temperature (PVT) equation-of-state (EOS) relationship as expressed through the solubility of a blowing agent in a polymer melt is at the heart of the design and prediction of polymeric foams, particularly for micro- and nanocellular foams, where the voids are on the order of microns and nanometers, respectively. These more-advanced foams represent existing or emerging materials for higher-value and high-technology applications.

As a route to understanding the important physics of the inhomogeneous structures of nanocellular polymeric foams, self-consistent field theory (SCFT) has been applied to investigate surface tension [2,3], the limitations of classical nucleation theory [4], and thermodynamic limits on cell densities [5,6]. The aforementioned work was done on a qualitative basis due to a number of limiting theoretical factors, one of which is the nature of the underlying EOS embedded in SCFT. Compressibility was included in the SCFT approach using the method of Hong and Noolandi [7], by which they showed that SCFT reduces to the Sanchez-Lacombe (SL) EOS. As such, an understanding of the SL EOS is required for understanding the behaviors of polymer foams, as described by SCFT, as well as fundamentally in terms of the solubility of the blowing agent in a homogeneous polymer melt.

In 1974, Sanchez and Lacombe introduced a lattice-based statistical mechanical theory to describe fluid-phase equation-of-state behavior. Their original short paper [8] was soon followed by more-detailed descriptions for both pure fluids [9,10] and mixtures [11,12]. This theory, known as the lattice-fluid model, or the SL EOS, relies on vacancies or “holes” to account for compressibility and, due to its

*thompson@uwaterloo.ca

simplicity, continues to be widely used in everything from hydrogen storage applications [13] to efforts to understand dark energy [14]. Applications to polymer systems are the most common, however, and the theory has been widely applied to polymeric foams.

Among polymers, polypropylene (PP) is one of the most widely used commodity polymers, with carbon dioxide (CO₂) often chosen as an environmentally friendly blowing agent for the manufacture of polymeric foams [15–19]. The advent of the experimental ability to independently measure both solubilities and swelling has shown the SL EOS to perform poorly for these measurements, even when the mixture parameters are allowed to change with temperature and pressure [15,17,18,20]. Within the context of the statistical mechanical derivation of the SL EOS, these mixture parameters should be constant. There are, however, a number of confounding factors. The SL EOS for mixtures requires as input the parameters for the pure components—poor estimates for the pure-component parameters will lead to poor agreement with experiment for mixtures [21]. Also, at coexistence, the SL EOS is often solved analytically, requiring rather severe approximations which can corrupt the agreement with experiment [22,23]. These approximations can be somewhat compensated for in certain circumstances [24]. Lastly, the SL EOS for mixtures has been shown to be thermodynamically inconsistent due to the mixing rules used to set the volume of the holes [25]. This issue goes deeper than is presently appreciated.

In this paper, we rederive the SL EOS using an off-lattice formalism in order to show that the limitations of the SL EOS do not arise from the lattice. We also find the approach to be particularly simple, as it follows the spirit of the SCFT derivation of Hong and Noolandi [7], but without the path-integral formalism required to describe inhomogeneous systems. We show the inconsistency that arises from the so-called mixing rules, originally noticed by Neau [25], but we demonstrate this inconsistency from an additional perspective and show that the fugacity coefficients suggested by Neau do not remove the inconsistency. In fact, we are not presently aware of any way to remove the inconsistency for any choice of mixing rules. Nonetheless, the theory can be shown to be reliable in the context of coexistence calculations, where we will show mixing rules to be unnecessary. Rather, constant hole volumes allow the SL EOS to be near consistent for solubility calculations. At coexistence, we find excellent agreement with experimental solubilities for a mixture of PP and CO₂ using a constant hole volume and without changing the mixture parameters with temperature or pressure. We are careful in obtaining the best possible values for the pure-component parameters—we regress new characteristic parameters for both linear and branched PP to known data formulas and use parameters from our previous in-depth study of CO₂ [26]. It is shown, however, that not all three pure-component parameters for PP are needed. One can be ignored due to the corresponding-states

principle of the SL EOS, and another due to the avoidance of mixing rules. Without mixing rules, the agreement with PP-CO₂ experiment is much better than for the SL EOS, with typical mixing rules based on the same parameters and methods. We also predict the swelling at saturation with no further free parameters. The agreement with experiment here is worse, but still better than mere order of magnitude. We offer an explanation of the worse fit for swelling based on the difference in hole size between the polymer and CO₂ molecules, which causes the inherent inconsistency of the SL EOS to be more pronounced for that calculation. We go on to consider an empirical relationship between the holes and missing correlations and show that the differing SL-EOS parameters for pure linear PP and pure branched PP become very similar when the parameters are made independent of the hole size. Lastly, we are able to extract a rough estimate of the single required pure-component PP SL-EOS parameter from the solubility data, along with the usual mixture parameters. Thus, we demonstrate the predictive nature of our approach and its applicability to systems where the pure-component parameters of a substance are not known. This offers a potentially better and simpler alternative to approaches such as the group-contribution method [13,27] and extends predictive capability to a wider range of polymeric foams.

II. THEORY

The idea behind the SL EOS is to represent free volume as discrete vacancies, or holes, that behave as an additional chemical species in terms of translational entropy, but that have no interactions or internal degrees of freedom. The artificial translational entropy is adjusted, through a change of hole size, so that the equation of state correctly describes the density behavior of the pure-component substance or mixture. Here, we give an off-lattice derivation that is equivalent to the SL EOS, together with a different treatment of mixture holes.

The canonical partition function for a multiple-chemical-species system—consisting of n_κ molecules of species κ and n_0 artificial holes that, combined, fill all space—is given by

$$\mathcal{Q} = \frac{1}{\prod_\kappa n_\kappa! \Lambda_\kappa^{3n_\kappa}} \int \prod_\kappa^0 d\{\mathbf{r}_\kappa\} e^{-V(\{\mathbf{r}_{\kappa \neq 0}\})/k_B T}, \quad (1)$$

where products (and, later, sums) are over all species κ , with the superscript 0 indicating that holes are included as a species, whereas products (or sums) without the superscript 0 indicate that holes are not included. Λ_κ 's where $\kappa \neq 0$ are de Broglie wavelengths containing the kinetic-energy contributions of all degrees of freedom of molecules of species κ , and Λ_0 is a normalization factor for the holes such that the partition function remains dimensionless. The sets of positions of the centers of mass of molecules of

species κ are given by $\{\mathbf{r}_\kappa\}$. The total potential $V(\{\mathbf{r}_{\kappa \neq 0}\})$ depends on the positions of all molecules of all species, but not on the positions of the holes. k_B is Boltzmann's constant and T is the temperature. The potential will, in general, be a very complicated function which, in principle, should also depend on other degrees of freedom of the molecules. If one divides the molecules up arbitrarily into N_κ segments of volume v_κ each, such that a single molecule of species κ has a total volume of $N_\kappa v_\kappa$, one can instead write the partition function in terms of a potential $U(\{\mathbf{r}_{s,\kappa \neq 0}\})$ based on the set of the positions of all of the segments $\{\mathbf{r}_{s,\kappa \neq 0}\}$ of all molecules of all species excluding holes, rather than the molecular centers of mass. Note that each hole is defined with $N_0 = 1$ so that v_0 is the volume of a hole. The partition function is then

$$Q = \frac{1}{\prod_\kappa n_\kappa! \Lambda_\kappa^{3n_\kappa}} \int \prod_\kappa d\{\mathbf{r}_\kappa\} e^{-U(\{\mathbf{r}_{s,\kappa \neq 0}\})/k_B T}, \quad (2)$$

where the segment distribution $\{\mathbf{r}_{s,\kappa \neq 0}\}$ is dependent on the molecular centers of mass $\{\mathbf{r}_{\kappa \neq 0}\}$ that we are integrating over. The particular relationship between molecular centers of mass and segment positions will depend on the details of the molecular model. For example, for inhomogeneous polymer systems, self-consistent field theory is used to compute molecular volume fractions for Gaussian strings in the mean-field approximation [4–6,28,29].

Instantaneous segment volume-fraction operators can be defined for all κ chemical species, as well as holes, as

$$\hat{\phi}_\kappa(\mathbf{r}) = v_\kappa \sum_{i=1}^{N_\kappa n_\kappa} \delta(\mathbf{r} - \mathbf{r}_{s,i}), \quad (3)$$

where $\mathbf{r}_{s,i}$ is the position of the i th segment, and the sum runs over all segments of all molecules of species κ . The various volumes of segments of different species v_κ are, in general, different, including the volume of a hole v_0 . In terms of these volume-fraction operators, the constraint that molecular segments plus holes fill all space can be phrased simply as

$$\sum_\kappa \hat{\phi}_\kappa(\mathbf{r}) = 1. \quad (4)$$

Assuming only pairwise interactions between segments, the potential $U(\{\mathbf{r}_{s,\kappa \neq 0}\})$ can be written in terms of volume-fraction operators as

$$U(\{\mathbf{r}_{s,\kappa \neq 0}\}) = \frac{1}{2} \sum_{\kappa \kappa'} \frac{1}{v_\kappa v_{\kappa'}} \int d\mathbf{r} d\mathbf{r}' \hat{\phi}_\kappa(\mathbf{r}) u_{\kappa \kappa'}(|\mathbf{r} - \mathbf{r}'|) \hat{\phi}_{\kappa'}(\mathbf{r}'), \quad (5)$$

where $u_{\kappa \kappa'}(\mathbf{r})$ is the segment-segment pair potential and self-energies are ignored [30]. Using this form of the potential in Eq. (2) gives

$$Q = \frac{1}{\prod_\kappa n_\kappa! \Lambda_\kappa^{3n_\kappa}} \int \prod_\kappa d\{\mathbf{r}_\kappa\} \times e^{-(1/2) \sum_{\kappa \kappa'} (1/v_\kappa v_{\kappa'}) \int d\mathbf{r} d\mathbf{r}' \hat{\phi}_\kappa(\mathbf{r}) u_{\kappa \kappa'}(|\mathbf{r} - \mathbf{r}'|) \hat{\phi}_{\kappa'}(\mathbf{r}')/k_B T}, \quad (6)$$

subject to the constraint (4).

The SL EOS is a mean-field and homogeneous theory, which, in the present context, can be incorporated using

$$\phi_\kappa \equiv \frac{1}{V} \int d\mathbf{r} \langle \hat{\phi}_\kappa(\mathbf{r}) \rangle = \frac{1}{V} \int d\mathbf{r} \hat{\phi}_\kappa(\mathbf{r}), \quad (7)$$

where $\langle \hat{\phi}_\kappa(\mathbf{r}) \rangle$ are ensemble average segment volume fractions and V is the system volume in the canonical ensemble. Replacing the instantaneous volume fractions, which depend on the segment positions, with the homogeneous mean-field volume fractions, which do not, means that Eq. (6) becomes

$$Q = \prod_\kappa \frac{V^{n_\kappa}}{n_\kappa! \Lambda_\kappa^{3n_\kappa}} e^{-(1/2) \sum_{\kappa \kappa'} (\phi_\kappa \phi_{\kappa'} / v_\kappa v_{\kappa'}) \int d\mathbf{r} d\mathbf{r}' [u_{\kappa \kappa'}(|\mathbf{r} - \mathbf{r}'|)/k_B T]}, \quad (8)$$

which is now subject to the homogeneous mean-field constraint

$$\sum_\kappa \phi_\kappa = 1. \quad (9)$$

We define a spatially averaged interaction parameter,

$$\epsilon_{\kappa \kappa'} = -\frac{v_r}{V} \frac{1}{2v_\kappa v_{\kappa'}} \int d\mathbf{r} d\mathbf{r}' u_{\kappa \kappa'}(|\mathbf{r} - \mathbf{r}'|), \quad (10)$$

with a factor v_r/V , where v_r is an arbitrary reference volume, included for later convenience, and a minus sign, also for convenience, so that positive values of $\epsilon_{\kappa \kappa'}$ will lower the free energy and contribute to the cohesion of the substance. Note that, assuming the pair interaction potential is not long-range, one can confirm that definition (10) is a constant with respect to volume. The approximate partition function (8) becomes

$$Q = \prod_\kappa \frac{V^{n_\kappa}}{n_\kappa! \Lambda_\kappa^{3n_\kappa}} e^{(V/v_r) \sum_{\kappa \kappa'} \phi_\kappa \phi_{\kappa'} (\epsilon_{\kappa \kappa'} / k_B T)}, \quad (11)$$

subject to Eq. (9).

The Helmholtz free energy is obtained in the usual way from the canonical partition function through $F = -k_B T \ln Q$. From Eq. (11), we get a dimensionless free energy of

$$\frac{F}{k_B T} = -\frac{V}{v_r} \sum_{\kappa \kappa'} \frac{\epsilon_{\kappa \kappa'}}{k_B T} \phi_\kappa \phi_{\kappa'} + \sum_\kappa \left[n_\kappa \ln \left(\frac{n_\kappa \Lambda_\kappa^3}{V} \right) - n_\kappa \right] \quad (12)$$

using Stirling's approximation. The first summations on the right-hand side are the summed energies of the molecular segment interactions. The subsequent terms are the translational entropies of the molecules and holes. These are the only physical aspects present in the SL EOS—all other properties are mapped to phenomenological parameters. In order to simplify later formulas, we can note that factors linear in n_κ will not affect any physical quantities derived from the free energy, so we add a factor,

$$n_\kappa \left[\ln \left(\frac{N_\kappa v_\kappa}{\Lambda_\kappa^3} \right) + 1 \right],$$

to the right-hand side of Eq. (12) and it becomes

$$\begin{aligned} \frac{F}{k_B T} = & -\frac{V}{v_r} \sum_{\kappa\kappa'} \frac{\epsilon_{\kappa\kappa'}}{k_B T} \phi_\kappa \phi_{\kappa'} + \left[n_0 \ln \left(\frac{n_0 \Lambda_0^3}{V} \right) - n_0 \right] \\ & + \sum_{\kappa} n_\kappa \ln \left(\frac{n_\kappa N_\kappa v_\kappa}{V} \right). \end{aligned} \quad (13)$$

Note that terms linear in n_0 *cannot* be manipulated because n_0 is a function of both volume and particle numbers n_k through incompressibility. In particular, v_0 , which contributes to the value of n_0 through incompressibility, is usually taken to be a function of n_k ; that is, it is often defined through mixing rules.

This free energy can be seen to generate the SL EOS using the usual relation,

$$P = - \left(\frac{\partial F}{\partial V} \right)_{\{n_k\}, T}. \quad (14)$$

Using Eq. (14), Eq. (13) gives a dimensionless pressure of

$$\begin{aligned} \frac{v_r P}{k_B T} = & - \sum_{\kappa} \left(\frac{1}{\alpha_0} - \frac{1}{\alpha_\kappa} \right) \phi_\kappa - \frac{1}{\alpha_0} \ln \phi_0 - \sum_{\kappa\kappa'} \frac{\epsilon_{\kappa\kappa'}}{k_B T} \phi_\kappa \phi_{\kappa'} \\ & + \frac{1}{\alpha_0} \left[1 - \ln \left(\frac{\Lambda_0^3}{v_0} \right) \right], \end{aligned} \quad (15)$$

where we use the fact that $\phi_\kappa = n_\kappa N_\kappa v_\kappa / V$ and that $n_0 = n_0(V)$ due to Eq. (9); that is, for a given hole volume v_0 , the number of holes must be chosen to fill all empty space. In Eq. (15), we define

$$\alpha_\kappa \equiv \frac{N_\kappa v_\kappa}{v_r} \quad (16)$$

as the ratio of a molecular volume to the reference volume. This definition is also taken to hold for the holes, where $\alpha_0 = v_0 / v_r$. Equation (15) is subject to the constraint (9).

Equation (15) can be shown to be equivalent to the SL EOS if we define the appropriate scaled quantities. The scaled density is defined as

$$\tilde{\rho} \equiv \sum_{\kappa} \phi_\kappa, \quad (17)$$

which allows us to define a species-averaged interaction energy,

$$\epsilon^* \equiv \frac{1}{\tilde{\rho}^2} \sum_{\kappa\kappa'} \epsilon_{\kappa\kappa'} \phi_\kappa \phi_{\kappa'}. \quad (18)$$

Using Eq. (18), we define a scaled pressure as

$$\tilde{P} \equiv \frac{v_r P}{\epsilon^*} \quad (19)$$

so that Eq. (15) becomes

$$\begin{aligned} \tilde{P} = & -\tilde{\rho}^2 - \frac{k_B T}{\epsilon^*} \left\{ \frac{\tilde{\rho}}{\alpha_0} - \sum_{\kappa} \frac{\phi_\kappa}{\alpha_\kappa} + \frac{1}{\alpha_0} \ln(1 - \tilde{\rho}) \right. \\ & \left. - \frac{1}{\alpha_0} \left[1 - \ln \left(\frac{\Lambda_0^3}{v_0} \right) \right] \right\}, \end{aligned} \quad (20)$$

where we make use of the fact that $\phi_0 = 1 - \sum_{\kappa} \phi_\kappa$. We define the scaled temperature as

$$\tilde{T} \equiv \frac{k_B T}{\epsilon^*}, \quad (21)$$

so that Eq. (20) can be rewritten as

$$\begin{aligned} \tilde{\rho}^2 + \tilde{P} + \tilde{T} \left\{ \frac{1}{\alpha_0} \ln(1 - \tilde{\rho}) - \sum_{\kappa} \frac{\phi_\kappa}{\alpha_\kappa} + \frac{\tilde{\rho}}{\alpha_0} - \frac{1}{\alpha_0} \left[1 - \ln \left(\frac{\Lambda_0^3}{v_0} \right) \right] \right\} \\ = 0. \end{aligned} \quad (22)$$

An average molecular size r can be defined such that

$$\frac{1}{r} \equiv \frac{1}{\tilde{\rho}} \sum_{\kappa} \frac{\phi_\kappa}{\alpha_\kappa}, \quad (23)$$

and the equation of state becomes

$$\begin{aligned} \tilde{\rho}^2 + \tilde{P} + \tilde{T} \left\{ \left(\frac{1}{\alpha_0} - \frac{1}{r} \right) \tilde{\rho} + \frac{1}{\alpha_0} \ln(1 - \tilde{\rho}) - \frac{1}{\alpha_0} \left[1 - \ln \left(\frac{\Lambda_0^3}{v_0} \right) \right] \right\} \\ = 0. \end{aligned} \quad (24)$$

For the choice of a reference volume equal to the hole volume ($v_r = v_0$), we get $\alpha_0 = 1$, and Eq. (24) is the SL EOS with an extra term. The extra term is unphysical because, in the limit of $\tilde{\rho} \rightarrow 0$, we require the absolute pressure to go to zero, $\tilde{P} \rightarrow 0$. This is possible only if we set the hole normalization factor to $\Lambda_0^3 = v_0 e$, as suggested by Hong and Noolandi [7]. Then the equation of state is

$$\tilde{\rho}^2 + \tilde{P} + \tilde{T} \left[\left(\frac{1}{\alpha_0} - \frac{1}{r} \right) \tilde{\rho} + \frac{1}{\alpha_0} \ln(1 - \tilde{\rho}) \right] = 0, \quad (25)$$

which, for $v_r = v_0$, is the SL EOS.

Characteristic parameters ρ^* , P^* , and T^* can be defined following Sanchez and Lacombe [9], with $\tilde{\rho} = \rho/\rho^*$ (or, equivalently, $\tilde{\rho} = V^*/V$), $\tilde{P} = P/P^*$, and $\tilde{T} = T/T^*$. From Eq. (17), V^* is

$$V^* = \sum_{\kappa} n_{\kappa} N_{\kappa} v_{\kappa} = \sum_{\kappa} \alpha_{\kappa} v_r n_{\kappa} \quad (26)$$

using the definition of α_{κ} . Equation (26) can be phrased in terms of the mass density characteristic parameter ρ^* as

$$\rho^* = \frac{\sum_{\kappa} n_{\kappa} M_{\kappa}}{V^*}, \quad (27)$$

where M_{κ} is the molecular weight of species κ . Trivially, from Eqs. (19) and (21), P^* and T^* are

$$P^* = \frac{\epsilon^*}{v_r}, \quad (28)$$

$$T^* = \frac{\epsilon^*}{k_B}, \quad (29)$$

respectively. Equations (26), (27), (28), (29), (18), and (23) can be shown to be equivalent to Eqs. (17), (37), (25), (24), (27), and (32), respectively, of Ref. [11], provided that the reference volume v_r is taken to be the hole volume.

The mixture characteristic parameters can be divided into pure-component characteristic parameters [9] and interaction parameters [11]. For the volume expression (26), there are no cross terms, so one can define

$$V_{\kappa}^* = n_{\kappa} N_{\kappa} v_{\kappa} = \alpha_{\kappa} v_r n_{\kappa}, \quad (30)$$

which is the total volume occupied by molecules of type κ . The pure-component characteristic density is

$$\rho_{\kappa}^* = \frac{n_{\kappa} M_{\kappa}}{V_{\kappa}^*} = \frac{M_{\kappa}}{\alpha_{\kappa} v_r}. \quad (31)$$

Equation (18) can be rewritten as

$$\epsilon^* \equiv \frac{1}{\tilde{\rho}^2} \left[\sum_{\kappa \neq \kappa'} \epsilon_{\kappa \kappa'} \phi_{\kappa} \phi_{\kappa'} + \sum_{\kappa} \epsilon_{\kappa \kappa} \phi_{\kappa}^2 \right], \quad (32)$$

which allows us to define the pure-component characteristic temperatures as

$$T_{\kappa}^* = \frac{\epsilon_{\kappa \kappa}}{k_B}. \quad (33)$$

Rather than defining the interaction parameters directly from Eq. (32), we follow Lacombe and Sanchez [11] and

define a dimensionless interaction parameter as the deviation from the geometric mean of any two pure-component characteristic temperatures:

$$\zeta_{\kappa \kappa'} (T_{\kappa}^* T_{\kappa'}^*)^{1/2} = \frac{\epsilon_{\kappa \kappa'}}{k_B}, \quad \kappa \neq \kappa'. \quad (34)$$

Finally, the pure-component characteristic pressures can be written in the same way as the temperatures,

$$P_{\kappa}^* = \frac{\epsilon_{\kappa \kappa}}{v_r}. \quad (35)$$

No further binary interaction terms are required since P^* depends on ϵ^* in the same way that it does for the characteristic temperatures. A final parameter is v_0 , the hole volume. This is determined for pure-component systems by setting the reference volume equal to the hole volume and determining this hole volume by comparison to experiment. The hole volume will thus be different for each chemical species. For mixtures, the accepted approach is to define the hole volume using an arbitrary mixing rule that is a composition-dependent average of the various pure-component hole volumes. In this way, the hole volume will correctly limit to the known pure-component values.

For example, the original mixture SL EOS suggests a composition-based average such as [9]

$$v_0 = \frac{\sum_{\kappa} n_{\kappa} N_{\kappa} v_{0\kappa}}{\sum_{\kappa} n_{\kappa} N_{\kappa}}, \quad (36)$$

where $v_{0\kappa}$ is the hole volume for the pure-component species κ . For a binary mixture, this hole volume would be

$$v_0 = \frac{N_1 n_1 v_{01} + N_2 n_2 v_{02}}{N_1 n_1 + N_2 n_2}. \quad (37)$$

In order to account for deviations from this mixing rule, an arbitrary parameter δ is later added to give [31]

$$v_0 = \frac{N_1 n_1 v_{01} + N_2 n_2 v_{02}}{N_1 n_1 + N_2 n_2} - \frac{(N_1 n_1)(N_2 n_2)}{(N_1 n_1 + N_2 n_2)^2} \delta (v_{01} + v_{02}). \quad (38)$$

These rules are not derived but, rather, are arbitrary choices. Whether using these rules or others, the mixture SL EOS will necessarily be thermodynamically inconsistent, as can be shown via the chemical potentials.

The chemical potentials can be found from the free energy (13) using the relation

$$\mu_{\kappa} = \left(\frac{\partial F}{\partial n_{\kappa}} \right)_{T, V, n_{\kappa' \neq \kappa}} \quad (39)$$

for $\kappa \neq 0$. Making use of incompressibility (9) and the free-energy density, the dimensionless chemical potentials are

$$\frac{\mu_\kappa}{k_B T} = \alpha_\kappa \left[-\frac{1}{\alpha_0} + \frac{1}{\alpha_\kappa} (1 + \ln \phi_\kappa) - \frac{1}{\alpha_0} \ln \phi_0 - 2 \sum_{\kappa'} \frac{\epsilon_{\kappa\kappa'}}{k_B T} \phi_{\kappa'} + \frac{n_0}{v_0} \frac{\partial v_0}{\partial n_\kappa} \ln \phi_0 \right]. \quad (40)$$

This expression agrees with that of Hong and Noolandi [7] for $v_r = v_0$, except for the generalization to a nonconstant, composition-dependent hole volume given by the last term due to the assumption of mixing rules. This term disappears in the dilute limit, and the chemical potentials become

$$\lim_{\phi_\kappa \rightarrow 0} \frac{\mu_\kappa}{k_B T} = -\frac{N_\kappa v_\kappa}{v_0} + 1 + \ln \phi_\kappa. \quad (41)$$

These chemical potentials agree with ideal-gas expressions up to additive constants, except for the presence of v_0 . Since the hole volume will depend on the composition through mixing rules, the functional form of Eq. (41) will deviate from the ideal gas unless v_0 is constant. If v_0 is constant for a mixture, however, it cannot limit correctly to the pure components. Thus, a constant hole volume violates the pure-component limits, and a variable hole volume does not provide a consistent zero of energy for either the chemical potentials or the free energy. This fundamental inconsistency of the SL EOS was first reported by Neau [25].

Neau offers a solution to the inconsistency. She argues that the pressure derived from the configurational integral should be equal to the pressure arising from the full partition function since

$$\ln Q = \ln \lambda(n, T) + \ln Z(n, V, T), \quad (42)$$

where Q is the partition function, Z is the configurational integral, and λ represent normalization and kinetic-energy prefactors of the partition function. Since λ does not depend on volume, the pressure calculated using Eq. (14) should be the same for the configurational integral as for the full partition function. Neau suggested integrating P_{conf} to get a new free energy, which she then used to find chemical potentials which limit in the dilute case correctly [25]. However, uniquely for hole theories, an n_0 factor which must enter $\lambda(n_0, n, T)$ will depend on volume through incompressibility since the free volume is represented as another species filling all available space. This dependency on volume can be understood by rephrasing Eq. (9) for the incompressibility in terms of particle numbers instead of volume fractions using the relation

$$\phi_\kappa = \frac{n_\kappa N_\kappa v_\kappa}{V} \quad (43)$$

so that Eq. (9) becomes

$$n_0 = \frac{V - \sum_\kappa n_\kappa N_\kappa v_\kappa}{v_0}. \quad (44)$$

Thus, it can be seen that, for a hole theory, $\lambda(n_0, n, T) = \lambda(n_0(V), n, T)$. Since there is now a volume dependence in this prefactor term, $P_{\text{conf}} \neq P$ and the Neau argument is not valid. The fugacity coefficients she provided cannot, therefore, be used to correct the chemical potentials. The SL EOS remains inconsistent for all mixing rules except for constant hole volumes, in which case it cannot limit correctly to pure components.

There may be cases where limiting to pure-component hole volumes is not required or expected. For example, following the saturation line of a polymer–small molecule (polymer–solvent) mixture to approaching the pure solvent limit would imply reaching a condition of polymer in a vapor phase within the solvent liquid. This situation is unphysical for long polymer chains. Similarly, approaching the pure polymer state following the saturation line could be unphysical provided that the polymer solidifies before excluding most solvent from the polymer matrix. Thus, along the saturation line, one does not necessarily require the hole volume to limit to the pure components. Furthermore, as is evidenced in Sec. III, a constant hole volume along this line is able to produce excellent agreement with solubility experiments. An interpretation of this agreement in terms of an empirical correlation correction at saturation is also given in Sec. III.

Equilibrium calculations can, therefore, be attempted for such cases using the chemical-potential expressions (40) since these chemical potentials share a consistent energy zero for constant hole volumes. The pressure formula also limits correctly only for the choice of a constant hole volume, as can be shown by rederiving it using

$$-PV = F - \sum_\kappa \mu_\kappa n_\kappa \quad (45)$$

or, equivalently,

$$\frac{v_r P}{k_B T} = -\frac{v_r F}{V k_B T} + \sum_\kappa \frac{\mu_\kappa}{k_B T} \frac{n_\kappa v_r}{V}. \quad (46)$$

Equations (13) and (40) give a pressure expression of

$$\begin{aligned} \frac{v_r P}{k_B T} = & -\sum_\kappa \left(\frac{1}{\alpha_0} - \frac{1}{\alpha_\kappa} \right) \phi_\kappa - \frac{1}{\alpha_0} \ln \phi_0 - \sum_{\kappa\kappa'} \frac{\epsilon_{\kappa\kappa'}}{k_B T} \phi_\kappa \phi_{\kappa'} \\ & + \sum_\kappa \phi_\kappa \frac{n_0}{v_0} \frac{\partial v_0}{\partial n_\kappa} \ln \phi_0, \end{aligned} \quad (47)$$

where we use the previous result that $\Lambda_0^3 = v_0 e$. This result can be seen to agree with the pressure formula (15) provided that

$$\sum_{\kappa} \phi_{\kappa} \frac{n_0}{v_0} \frac{\partial v_0}{\partial n_{\kappa}} \ln \phi_0 = 0. \quad (48)$$

For dilute systems where $\phi_0 \rightarrow 1$, this condition is met. In general, however, we require

$$\sum_{\kappa} \phi_{\kappa} \frac{\partial v_0}{\partial n_{\kappa}} = 0, \quad (49)$$

subject to the boundary conditions that $v_0 = v_{0\kappa}$ for each pure-phase κ . There is no physically meaningful solution to this first-order partial-differential-equation boundary value problem since it is overdetermined. Therefore, regardless of the mixing rules chosen, the SL EOS will be inconsistent unless a constant hole volume is used.

Even when using a constant hole volume along the saturation line, some inconsistency is unavoidable due to the approximate nature of using artificial holes to capture equation-of-state effects. Returning to the polymer-solvent mixture example, for the mixture phase to be in equilibrium with the pure solvent phase at saturation, the chemical potentials of the mixture and the pure-component phases must be equal. The constant hole volume for the mixture phase differs from the constant hole volume for the pure-component phase, so the chemical-potential comparison is based on different zeros of energies. However, for the determination of solubilities, if the hole volume of the mixture is not too different from the hole volume of the pure component, one may hope for quantitatively reliable results. This similarity between hole volumes can be determined *a posteriori* by comparing the fitted mixture hole volume to the known pure-component hole volume. As is shown in Sec. III, excellent results are possible.

On the other hand, some quantities may not be adequately determined. Swelling ratios at saturation may also be computed, but they require hole volumes for the mixture, for the pure solvent phase, and for the pure polymer phase. Since the pure polymer hole volume will certainly not be similar to the pure solvent hole volume, one should anticipate significant inconsistencies. Nonetheless, even for swelling ratios at saturation, one can achieve order-of-magnitude results that are satisfactory.

Using a constant hole volume for mixtures, it is logical to make it the reference volume. From Eqs. (46), (40), and (13), we get

$$\begin{aligned} \frac{v_0 P}{k_B T} = & - \sum_{\kappa} \frac{\phi_{\kappa}}{\alpha_{\kappa}} \ln \phi_{\kappa} - \left(1 - \sum_{\kappa} \phi_{\kappa}\right) \ln \left(1 - \sum_{\kappa} \phi_{\kappa}\right) \\ & + \sum_{\kappa} \frac{\phi_{\kappa}^2}{\tilde{T}_{\kappa}} + \sum_{\substack{\kappa\kappa' \\ \kappa \neq \kappa'}} \frac{\phi_{\kappa} \phi_{\kappa'}}{\zeta_{\kappa\kappa'} (\tilde{T}_{\kappa} \tilde{T}_{\kappa'})^{1/2}} + \sum_{\kappa} \frac{\phi_{\kappa} \mu_{\kappa}}{\alpha_{\kappa} k_B T}, \quad (50) \end{aligned}$$

with

$$\begin{aligned} \frac{\mu_{\kappa}}{\alpha_{\kappa} k_B T} = & -1 + \frac{1}{\alpha_{\kappa}} (1 + \ln \phi_{\kappa}) - \ln \left(1 - \sum_{\kappa} \phi_{\kappa}\right) - \frac{2\phi_{\kappa}}{\tilde{T}_{\kappa}} \\ & - \sum_{\substack{\kappa' \neq \kappa \\ \zeta_{\kappa\kappa'}}} \frac{2\phi_{\kappa'}}{(\tilde{T}_{\kappa} \tilde{T}_{\kappa'})^{1/2}}. \quad (51) \end{aligned}$$

These are useful forms for calculating coexistence quantities. Note that, in Eqs. (50) and (51), the quantities α_{κ} now refer to the ratio of a molecular volume to the hole volume of the mixture, $\alpha_{\kappa} = N_{\kappa} v_{\kappa} / v_0$. The hole volume of the mixture and the binary mixture parameters $\zeta_{\kappa\kappa'}$ are not known and have to be regressed from mixture data—in our case, from solubility data. As input, we need the pure-component parameters T_{κ}^* and $\rho_{\kappa}^* = M_{\kappa} / N_{\kappa} v_{\kappa}$, usually regressed to pure-component PVT data. Note that the pure-component parameter P_{κ}^* is not directly needed to fit to solubility in the context of a constant mixture hole volume. Equations (50) and (51) are solved numerically, which proceeds as follows.

Assuming values of $\zeta_{\kappa\kappa'}$ and v_0 , one can choose values of μ_{κ} allowing one to solve the κ equations (51) for the set of volume fractions ϕ_{κ} . There are κ independent solution sets which include each κ -rich phase. The known ϕ_{κ} and μ_{κ} values are substituted into Eq. (50) for all phases—the resultant set of reduced pressures will, in general, not be equal. One input μ_{κ} value is varied, with the others held constant until the output pressures are equal, giving the ϕ_{κ} volume fractions in all phases at one point at saturation, that is, at equal pressures, chemical potentials, and temperatures. This process is repeated for the various values of the μ_{κ} that were previously held constant to generate the entire saturation region. In turn, this whole process is repeated for different choices of $\zeta_{\kappa\kappa'}$ and v_0 (through $\alpha_{\kappa} = N_{\kappa} v_{\kappa} / v_0$) until the predicted solubilities match the experimentally available data.

For a two-species mixture consisting of a long polymer such as PP and a small molecule such as CO₂ (the solvent), such as in a polymeric foaming system, the process is simplified since it is known that there will be no polymer vapor in the CO₂-rich phase at any pressure or temperature; that is, $\phi_{PP} = 0$ in the CO₂-rich phase. Thus, for a choice of μ_{PP} and μ_{CO_2} , one solves Eq. (51) for the polymer-rich phase only and compares the pressure (50) so calculated with the pure CO₂ pressure using μ_{CO_2} . One varies μ_{CO_2} until the pressures of the pure component and the mixture are equal. This process is repeated for all values of μ_{PP} to find the saturation line. Alternatively, since $\phi_{PP} = 0$, one can choose a desired pressure, solve Eqs. (50) and (51) for the CO₂ phase for ϕ_{CO_2} and μ_{CO_2} , and then, for the same pressure, solve Eqs. (50) and (51) again—this time for the mixture—for the unknowns ϕ_{PP} , ϕ_{CO_2} , and μ_{PP} . Again, the process is repeated for different choices of ζ and v_0 until the predicted solubilities match the experimentally available data. Furthermore, for long molecules, α_{κ} becomes very large and the regression becomes insensitive to its

value; that is, Eqs. (50) and (51) are independent of α_κ in the limit of a large α_κ . Therefore, only the single parameter T_κ^* is needed to characterize the polymer in the mixture.

If the characteristic parameters of the long polymer are not known, one may be able to extract sufficient information from the solubility data to make predictions outside the experimental range. As mentioned, P_κ^* is not needed for mixture calculations, and, for sufficiently long polymers, $\alpha_{PP} \rightarrow \infty$. This is the well-known corresponding-states principle of the SL EOS. Given that the parameters $\zeta_{\kappa\kappa'}$ and the mixture v_0 are constant across temperatures and pressures, one can perform a regression for *three* parameters instead of two: $\zeta_{\kappa\kappa'}$, the mixture v_0 , and T_{PP}^* . While this procedure does not fully characterize the pure-component polymer, one would, in principle, have enough information from limited experimental solubility data to make solubility predictions at other temperatures and pressures, albeit with limited accuracy.

From the known volume fractions of the mixture along the saturation line, and the volume fractions of the pure-component CO_2 , the solubility χ_κ of species κ in a mixture can be calculated according to

$$\chi_\kappa = \frac{M_\kappa \phi_\kappa / \alpha_\kappa}{\sum_{\kappa'} M_{\kappa'} \phi_{\kappa'} / \alpha_{\kappa'}}, \quad (52)$$

where all volume fractions are calculated in the mixture phase at saturation. Formula (52) is just an expression of the ratio of the mass of species κ with respect to the total mass of all species in the mixture. In this work, we take experimental solubility data and numerically regress the mixture hole volume based on known CO_2 and PP characteristic parameters using a Levenberg-Marquardt algorithm [32,33]. We also calculate swelling ratios for species κ along the saturation line according to

$$S_W = \frac{\phi_\kappa^{\text{pure}}}{\phi_\kappa^{\text{mix}}}. \quad (53)$$

Equation (53) is an expression of the ratio of the volume of the mixture phase to the volume of the pure polymer phase such that both exist at the same temperature and pressure and contain the same number of κ molecules.

III. RESULTS AND DISCUSSION

Solubility and swelling are two quantities of significance in polymeric foaming [24,34]. For physical blowing agents, the amount of blowing agent dissolvable in a polymeric matrix will greatly effect the formation of a polymeric foam upon the inducement of a thermodynamic instability, either through a temperature increase or a pressure drop. The rapid temperature or pressure variation causes a change of the solubility of the blowing agent in the polymer, allowing the foam to form. Swelling is a measure of the amount of expansion of the material with respect to the original

volume of the pure polymer before foaming. This is a property that is extremely important for applications of the foam. Equation-of-state knowledge of solubility and swelling resulting from various chemistries of polymer and blowing agent is therefore of high value in anticipating the cell density of the foam and its other properties. In this section, we compare experimental results for solubility and swelling with predictions of the SL EOS without mixing results, as described in Sec. II. We choose these two quantities because of their relevance to polymeric foaming.

Experimental data for solubility experiments at saturation for linear PP- CO_2 mixtures are taken from Hasan *et al.* [15] and are shown in Fig. 1. Theoretical fits based on regressions to the experimental solubility data are also shown in Fig. 1. The parameters used in the regressions are given in Tables I and II. Characteristic parameters for pure CO_2 were regressed by us in Ref. [26], whereas, for pure polypropylene, regressions were made to empirical formulas fit to experimental data [34]. For mixtures, all additional parameters are regressed by us. For a constant mixture hole volume $v_0^{\text{mix}} = 8.436 \times 10^{-24} \text{ cm}^3$ and a binary interaction parameter $\zeta = 1.110$, excellent agreement with the experimental data is achieved over all pressures and temperatures without changing any parameters. Comparing Tables I and II, we see that the pure CO_2 hole volume of $v_0^{\text{CO}_2} = 1.124 \times 10^{-23} \text{ cm}^3$ is relatively similar to the mixture hole volume, justifying the equilibrium solubility calculation between the mixture and pure CO_2 . By contrast, other mixing-rule-based regressions are less satisfactory, with both the one- and two-parameter SL EOSs performing worse than the present approach over the three isotherms for constant $\zeta_{1\text{SL}}$ and $\zeta_{2\text{SL}}$, $\delta_{2\text{SL}}$ parameters. The arbitrary nature of the mixing rules for the one- and two-parameter SL EOSs mean that there is not a physical basis for this behavior; rather, the deviation occurs mathematically because the zero of chemical potential is changing in an arbitrary way, as expressed through the mixing rules.

For the same value of ζ , rough agreement with the swelling data at saturation is achievable for a constant mixture hole volume. Figure 2 shows the experimental swelling data for linear PP- CO_2 mixtures together with theoretical predictions. Experimental data are again taken from Ref. [15], with additional data at 473 K taken from Ref. [35]. The constant-hole-volume approach consistently overestimates the swelling and, more importantly, fails to capture qualitatively the slight concavity of the experimental curve. Nonetheless, quantitatively, the present approach is better than mere order-of-magnitude agreement. The 2SL EOS is similar to the present approach at 453 K, but it becomes significantly worse at higher temperatures. Surprisingly, the 1SL EOS remains competitive at all temperatures, indicating that a quadratic modification to the original SL mixing rule is not an appropriate correction for this case. Given the poor performance of the 1SL EOS

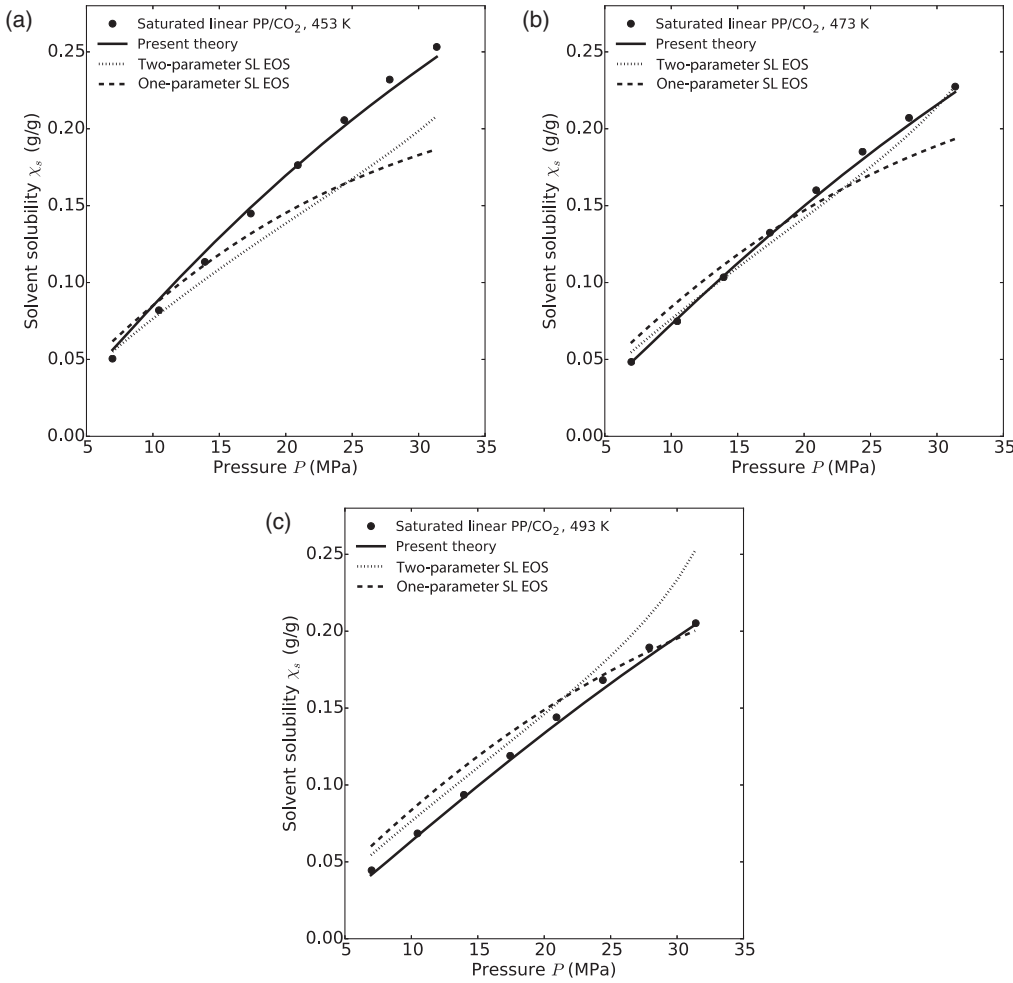


FIG. 1. Solubility data for linear PP-CO₂ mixtures at saturation at temperatures (a) 453 K, (b) 473 K, and (c) 493 K. Points indicate experimental data and lines display various theoretical fits denoted by the legends.

for solubilities, however, the present constant-hole-volume method gives the best overall performance, with the satisfactory swelling results arising without any free parameters. The difference in quality between the excellent solubility fits and the merely satisfactory swelling results can be understood in terms of the various hole volumes. Only the two relatively similar hole volumes $v_0^{\text{mix}} = 8.436 \times 10^{-24} \text{ cm}^3$ and $v_0^{\text{CO}_2} = 1.124 \times 10^{-23} \text{ cm}^3$ are required for the solubility, whereas, for swelling, the very different hole volume of pure linear PP with $v_0^{\text{PP}} = 2.894 \times 10^{-23} \text{ cm}^3$ enters the calculation. The swelling ratio should, in principle, be calculated by comparing

the PP-CO₂ mixture with the pure PP system under the same conditions, but the different hole volumes indicate a difference of the system chemical-potential zeros. Thus, we are, physically, calculating ratios of systems under different conditions, and one should thus not be surprised that the results are imperfect. By contrast, the qualitative agreement with experiment observed with the one-parameter SL theory in terms of the concavity of the swelling curve is unphysical, arising as it does through the arbitrary mixing rule. The one-parameter SL seems to capture this concavity trend through good fortune, which is borne out by the fact that, quantitatively, it is worse than our suggested approach. Overall, given the inherent inconsistency of all of the SL theories for nonconstant hole volumes, one should expect

TABLE I. Pure-component characteristic parameters and hole volumes from Ref. [26] for CO₂ and regressed from data of Ref. [34] for PP. The hole volumes are derived from the characteristic parameters according to $v_0 = k_B T^* / P^*$ [9].

| Molecule | T^* (K) | P^* (MPa) | ρ^* (g/cm ³) | v_0 ($\times 10^{-23} \text{ cm}^3$) |
|-----------------|-----------|-------------|-------------------------------|--|
| CO ₂ | 341.8 | 419.9 | 1.397 | 1.124 |
| Linear PP | 662.8 | 316.2 | 0.8685 | 2.894 |
| Branched PP | 656.0 | 356.4 | 0.8950 | 2.541 |

TABLE II. Mixture parameters for the present method (ζ , v_0), the two-parameter SL EOS ($\zeta_{2\text{SL}}$, $\delta_{2\text{SL}}$), and the one parameter SL EOS ($\zeta_{1\text{SL}}$).

| Mixture | ζ | v_0 ($\times 10^{-24} \text{ cm}^3$) | $\zeta_{2\text{SL}}$ | $\delta_{2\text{SL}}$ | $\zeta_{1\text{SL}}$ |
|-----------------------------|---------|---|----------------------|-----------------------|----------------------|
| Linear PP CO ₂ | 1.110 | 8.436 | 0.7244 | 0.1858 | 0.7571 |
| Branched PP CO ₂ | 1.091 | 8.646 | 0.7398 | 0.1728 | 0.7709 |

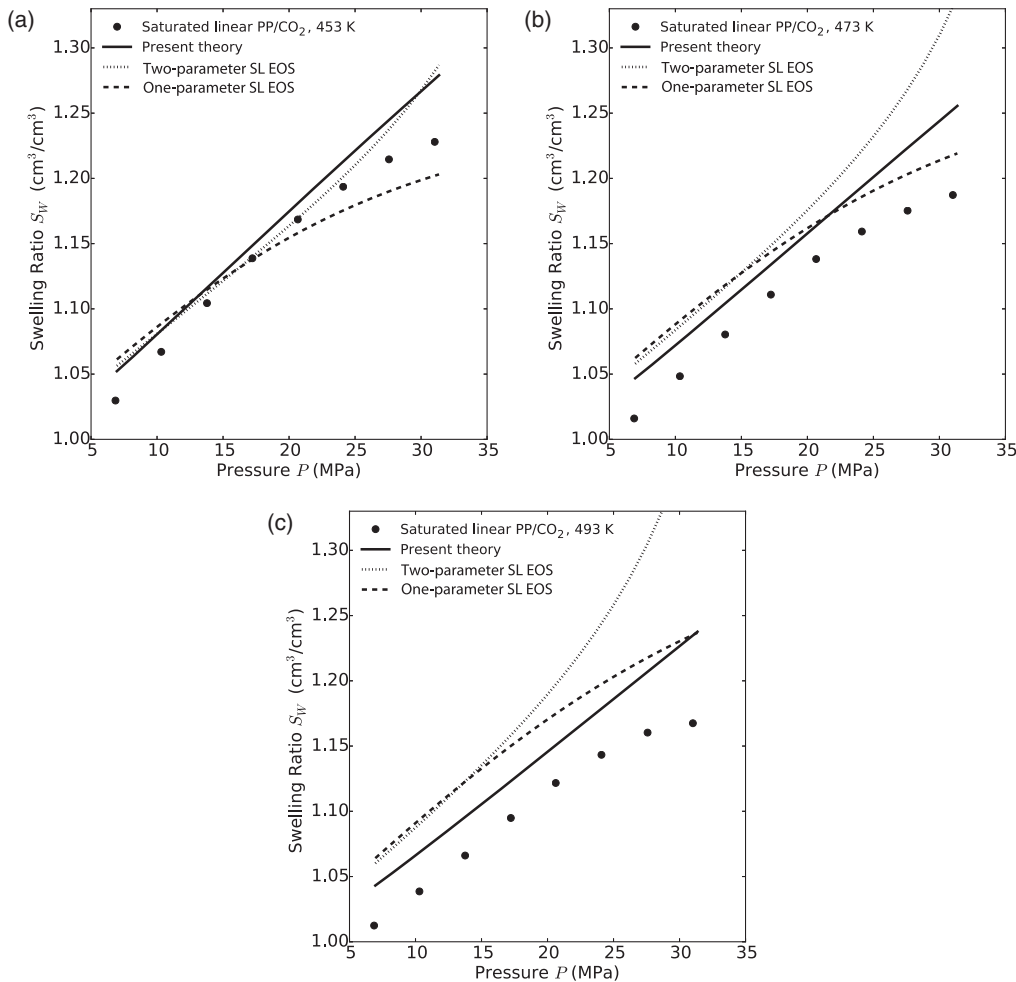


FIG. 2. Swelling data for linear PP-CO₂ mixtures at saturation at temperatures (a) 453 K, (b) 473 K, and (c) 493 K. Points indicate experimental data and lines display various theoretical fits denoted by the legends.

to have to use a more complicated EOS in order to improve the predictions for swelling.

Similar agreement for solubility and swelling at saturation is found for branched PP, using a hole volume of $v_0^{\text{mix}} = 8.646 \times 10^{-24} \text{ cm}^3$ and a binary interaction parameter of $\zeta = 1.091$, as shown in Figs. 3 and 4. Mixture data for branched PP is taken from Refs. [15,35]. Again, the constant-hole-volume fit does noticeably better than either the one- or the two-parameter SL-EOS fit, with excellent agreement for solubility and satisfactory agreement for swelling.

The surprisingly good performance of a constant hole volume for the mixtures can be interpreted in terms of an empirical correction to account for missing correlations. The SL EOS is mean-field theory, meaning that physically real correlations are not incorporated; on the other hand, holes, which are not physically real, are included in the SL EOS. One might wonder, then, if the holes can be roughly interpreted, in part, as an empirical correction for the missing correlations. For either a mixture or a pure-component substance, the holes are the gaps left behind as molecular segments—or groups of molecular segments—move about, exploring the phase space of a given statistical mechanical

ensemble. If the segments tend to move, on average, in correlated ways, then the size of the holes should reflect this. While the holes themselves are uncorrelated, the unit of discretized free space that is allowed to move around—that is, the hole size—forces a correlation among the movements of the remaining physical segments. In other words, the segments must move in “clumps” of a certain size. Of course, real correlations are, in principle, functions of temperature and pressure, with larger changes taking place near the critical point. If the neighborhood of the critical point is excluded from regressions, one might hope to represent these correlations approximately with a single empirical value—that is, the volume of a hole. One therefore expects the volume of holes to be different in various pure substances and in mixtures. There are a number of consequences in interpreting a hole in this way. First, at very low densities, nearing the ideal gas, the holes will be the dominant species filling most space, and the correlation interpretation will break down. From this point of view, one does not expect the SL EOS to be valid at very low densities. The thermodynamic inconsistency in the SL EOS was first shown by Neau by taking a low-density limit [25]—see Eq. (41). If the SL EOS is not valid in the dilute region, an

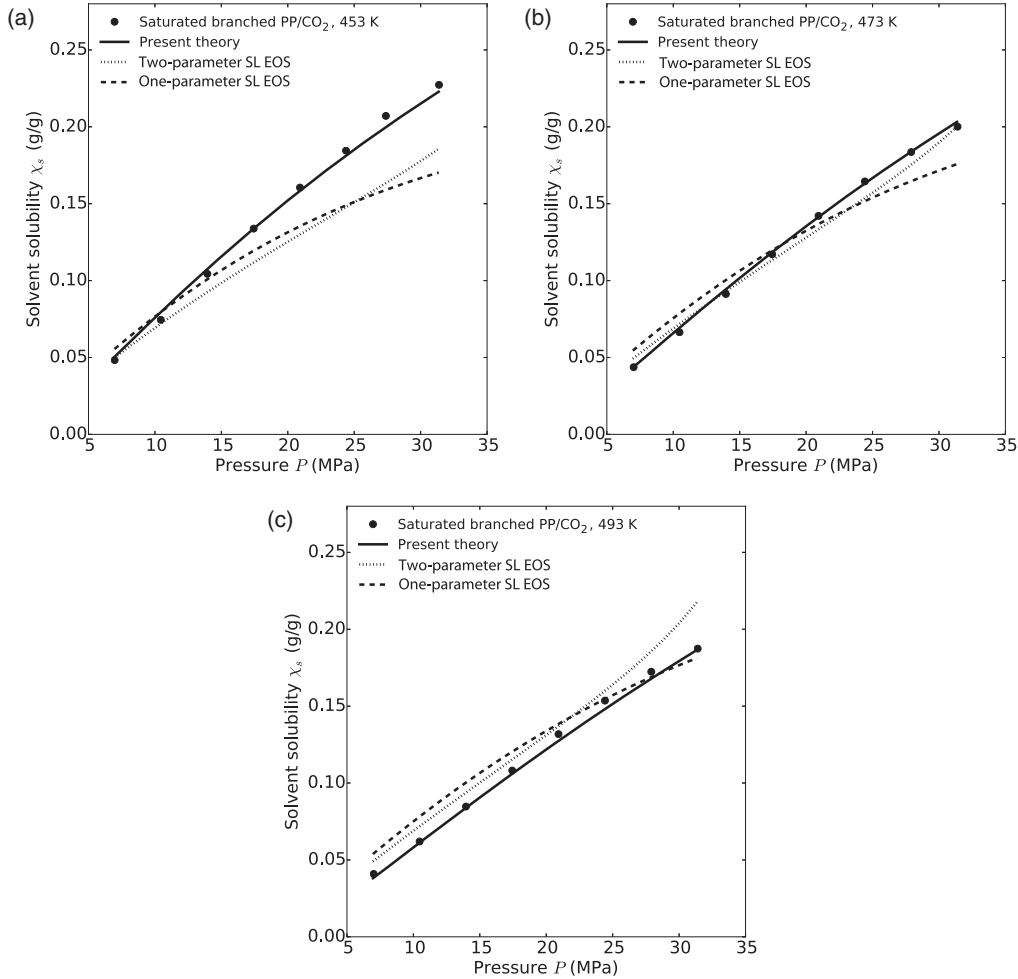


FIG. 3. Solubility data for branched PP-CO₂ mixtures at saturation at temperatures (a) 453 K, (b) 473 K, and (c) 493 K. Points indicate experimental data and lines display various theoretical fits denoted by the legends.

inconsistency there is not surprising. Nonetheless, as we have shown here—see Eq. (49)—the dilute limit merely illustrates an inconsistency that is present at all densities. Second, if hole volumes are viewed as empirical estimates of correlations, pure-component parameters must be functions of molecular architecture. Normally, in the SL EOS, pure-component parameters are, in principle, supposed to be the same for all molecular variations of a given substance. This expected consistency of parameters can be seen from the derivation in Sec. II, or the original lattice derivation [9], in which no segment connectivity information is retained. In reality, a consistency of pure-component parameters for different molecular architectures is rarely found. For example, branched and linear PP should have the same pure-component parameters. From Table I, we can see this is not so. While T^* and ρ^* are reasonably consistent with variations of between 1% and 3%, P^* varies on the order of 11%. From Eqs. (31), (33), and (35), it can be seen that, for a pure component with a reference volume equal to the hole volume ($v_r = v_0$), only the pressure characteristic parameter depends on the hole volume. If the hole volume represents correlations, we would expect to get different hole volumes between linear and branched PP since the architectural

differences will cause different segment motions and groupings as the phase space is explored. Thus, a different value of P^* is expected between linear and branched PP, while T^* and ρ^* should be similar. On the other hand, from formula (35), the product P^*v_0 is independent of the hole volume, so this product should be the same between linear and branched PP. From Table I, we find that this product changes only on the order of 1% between linear and branched PP, consistent with the small changes found for T^* and ρ^* . This finding provides evidence in support of interpreting the holes empirically to account for some correlations. Note that this discussion is not intended to be a rigorous proof that holes represent correlations—which, strictly speaking, they do not—but rather that the holes, as a phenomenological feature, are particularly well suited to incorporating missing correlations within an empirical parameter.

As mentioned in Sec. II, only one of the three characteristic parameters for PP, specifically, T_{PP}^* , is needed to fit to the solubility data with CO₂ when using a constant hole volume for the mixture. If this characteristic parameter is unknown, one could attempt to regress it together with v_0 and ζ from the solubility data. Figure 5 shows such fits to solubility data at 453 K for both branched and linear PP.

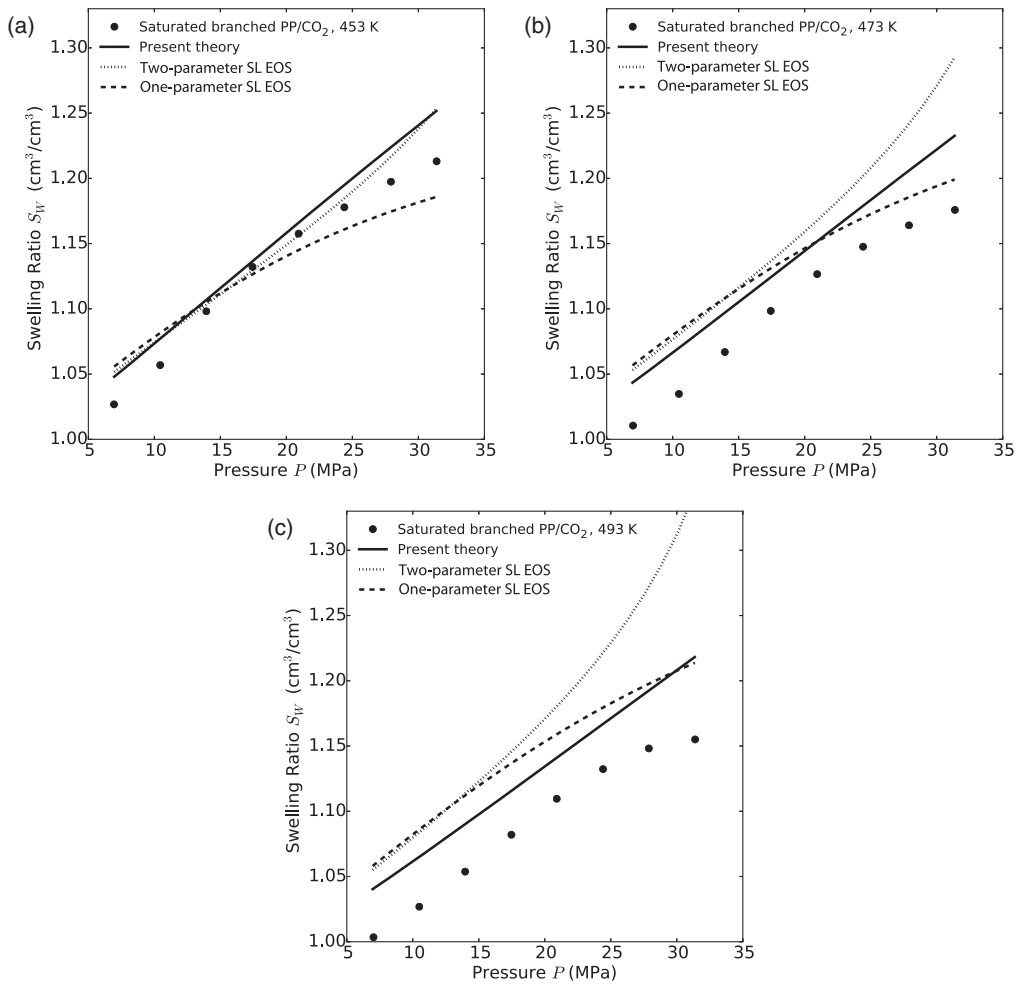


FIG. 4. Swelling data for branched PP-CO₂ mixtures at saturation at temperatures (a) 453 K, (b) 473 K, and (c) 493 K. Points indicate experimental data and lines display various theoretical fits denoted by the legends.

The values of the various regressed parameters are given in Table III. The values of ζ and v_0 for the mixture have changed with respect to the known T_{pp}^* case, as indicated by the percentages in parentheses in Table III, as has the prediction of T_{pp}^* . Some of this change is due to fitting to less data—that is, to 453 K only, rather than to all three temperatures—but most of it is due to the removal of the

constraint that T_{pp}^* should satisfy the pure PP PVT data. Despite the large change in T_{pp}^* (29% in the case of linear PP; the much smaller 3% change for branched PP is just fortuitous), the parameters from Table III can be used effectively for predictions. Figure 5 shows comparisons to solubility data at temperature of 473 and 493 K using only the parameters regressed to data at 453 K. The excellent

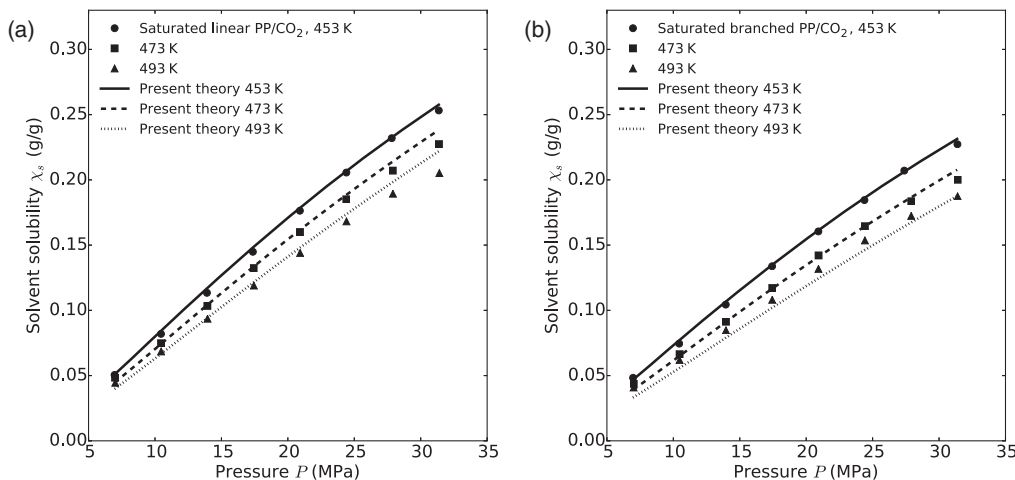


FIG. 5. Solubility data for (a) linear and (b) branched PP-CO₂ mixtures at saturation at temperatures of 453, 473, and 493 K, as denoted by the legends. Points indicate experimental data and lines display theoretical fits for parameters ζ , v_0 , and T_{pp}^* regressed at 453 K.

TABLE III. Mixture parameters for the present method (ζ , v_0) assuming that the parameter T_{pp}^* is also unknown and is regressed from the mixture. The percentages in parentheses indicate changes in values with respect to Tables I and II, where T_{pp}^* is known from pure-component data.

| Mixture | ζ | v_0 ($\times 10^{-24}$ cm ³) | T_{pp}^* |
|-----------------------------|------------|---|-------------|
| Linear PP CO ₂ | 1.039 (6%) | 7.745 (8%) | 470.4 (29%) |
| Branched PP CO ₂ | 1.115 (2%) | 7.719 (11%) | 639.3 (3%) |

agreement indicates that, operationally, the constant-hole-volume approach for mixtures at coexistence can provide information beyond the experimentally available data even when a large molecule component is completely uncharacterized. Even when extrapolating very far from the data range, one might still hope for reliable qualitative or order-of-magnitude predictions.

IV. CONCLUSIONS

An off-lattice statistical mechanical derivation of the SL EOS offers a simple approach for achieving the same result as the lattice-based method, regardless of the mixing rules chosen. The off-lattice result shows that issues of thermodynamic inconsistency are not artifacts of the lattice, and it further shows that fugacity coefficients cannot be used to correct the inconsistencies as previously believed [25]. Instead, one may choose to abandon the requirement that the mixture hole volume should reduce to the pure-component hole volumes, which allows the use of a constant hole volume for the mixture. For coexistence calculations involving PP and CO₂, this is shown to be a reasonable approach since, at coexistence, one does not expect to find the mixture phase limiting to either pure PP or pure CO₂. Furthermore, it is found that the hole volume for the pure CO₂ phase is close to the value of the hole volume for the PP-CO₂ mixture phase at coexistence, justifying *a posteriori* near consistency for this case. One might expect similar results for other polymer-small molecule systems at coexistence, with a comparison of mixture and pure small molecule hole volumes providing evidence as to whether the approach is indeed applicable in each case. In this work, the mixture hole volume is regressed from solubility data, whereas the pure CO₂ hole volume is taken from previous data [26].

One might speculate that the similarity of hole volumes at coexistence between PP and CO₂ arises from a similarity of correlations at coexistence. We discuss this as a possible physical interpretation of the holes based on the picture that molecular segments moving together in correlated ways will, on average, leave vacancies behind them that will differ in size from uncorrelated systems. In support of this interpretation, we observe that, although linear PP and branched PP have different pure-component P^* parameters, this parameter is dependent on the hole size. Because of the

differing architectures of linear and branched PP, one would expect different correlations, and thus different hole sizes and P^* parameters. Indeed, removing the hole volume from the definition of P^* gives very similar quantities for both linear and branched PP. For completeness, all three pure PP parameters are given in Table I.

Using a constant hole volume for the mixture instead of using mixing rules not only simplifies the theory but also gives better agreement with solubility experiments than using typical mixing rules. Although swelling ratios at saturation agree less well with experiment than for solubilities, the results are still satisfactory given that no free parameters are left in the comparison. It also makes sense that swelling predictions should be worse than solubility since, for swelling, the hole volume for pure PP is required, and it is very different from either the pure CO₂ hole volume or the PP-CO₂ mixture hole volume. Nonetheless, the swelling predictions using a constant hole volume are also better than when using mixing rules. Solubility and swelling measurements are of high significance to polymeric foaming, which is the focus of this paper, but the constant-hole-volume approach could be used for other coexistence quantities provided that the magnitudes of the differences in hole volumes between the constituents required for the particular coexistence property of interest are not too large.

In all cases, the binary fitting parameters used for solubility fitting, ζ and v_0 , do not need to be—and indeed should not be—varied with temperature or pressure. This means that, at coexistence, the use of a constant hole volume for mixtures provides a quantitatively predictive approach across temperatures and pressures based on a limited set of solubility data. Given the constancy of the mixture parameters, one can also attempt to regress the pure-component parameters of one species if that data are lacking. Operationally, only one pure-component parameter is needed for long polymers. The hole volumes of the pure components are not needed for the mixture since those hole volumes correspond to correlations in the pure component, and the mixture hole volume is considered to be constant and independent of them. Thus, the pure component P^* is not needed for the solubility regression. Furthermore, for long polymers such as the PP studied here, the corresponding-states principle of the SL EOS means that, effectively, the ρ^* of the pure components is not needed either. For the pure CO₂ phase, these parameters are, of course, still required, but there is no pure PP phase at coexistence, so one can do the solubility regression to extract ζ , v_0 , and T_{pp}^* . Although this regression does not produce extremely accurate results for the parameters themselves, the predicted results for PP-CO₂ solubilities are in excellent agreement with the experiments. In other words, variations in T_{pp}^* are counterbalanced by nonlinear variations in $\zeta_{\kappa\kappa'}$ and/or v_h . The predicted solubilities seem far better than what one might expect from using

techniques such as group-contribution theory [13,27]. Thus, the SL EOS using a constant hole volume for mixtures shows great promise for coexistence predictions for both industrially relevant systems such as polymeric foams and exotic systems where the pure-component parameters of one component may not be known.

ACKNOWLEDGMENTS

This research was financially supported by the Natural Sciences and Engineering Research Council of Canada (NSERC) as well as the Consortium for Cellular and Microcellular Plastics (CCMCP).

-
- [1] S.-T. Lee, C. B. Park, and N. S. Ramesh, *Polymeric Foams: Science and Technology* (CRC Press, Boca Raton, 2007).
- [2] H. Park, R. B. Thompson, N. Lanson, C. Tzoganakis, C. B. Park, and P. Chen, Effect of temperature and pressure on surface tension of polystyrene in supercritical carbon dioxide, *J. Phys. Chem. B* **111**, 3859 (2007).
- [3] R. B. Thompson, J. R. MacDonald, and P. Chen, Origin of change in molecular-weight dependence for polymer surface tension, *Phys. Rev. E* **78**, 030801 (2008).
- [4] Y. Kim, C. B. Park, P. Chen, and R. B. Thompson, Origins of the failure of classical nucleation theory for nanocellular polymer foams, *Soft Matter* **7**, 7351 (2011).
- [5] Y. Kim, C. B. Park, P. Chen, and R. B. Thompson, Towards maximal cell density predictions for polymeric foams, *Polymer* **52**, 5622 (2011).
- [6] Y. Kim, C. B. Park, P. Chen, and R. B. Thompson, Maximal cell density predictions for compressible polymer foams, *Polymer* **54**, 841 (2013).
- [7] K. M. Hong and J. Noolandi, Conformational entropy effects in a compressible lattice fluid theory of polymers, *Macromolecules* **14**, 1229 (1981).
- [8] I. C. Sanchez and R. H. Lacombe, Theory of liquid-liquid and liquid-vapour equilibria, *Nature (London)* **252**, 381 (1974).
- [9] I. C. Sanchez and R. H. Lacombe, An elementary molecular theory of classical fluids. Pure fluids, *J. Phys. Chem.* **80**, 2352 (1976).
- [10] I. C. Sanchez and R. H. Lacombe, An elementary equation of state for polymer liquids, *J. Polym. Sci., Polym. Lett. Ed.* **15**, 71 (1977).
- [11] R. H. Lacombe and I. C. Sanchez, Statistical thermodynamics of fluid mixtures, *J. Phys. Chem.* **80**, 2568 (1976).
- [12] I. C. Sanchez and R. H. Lacombe, Statistical thermodynamics of polymer solutions, *Macromolecules* **11**, 1145 (1978).
- [13] S. J. Alesadi and F. Sabzi, Hydrogen storage in a series of Zn-based MOFs studied by Sanchez-Lacombe equation of state, *Int. J. Hydrogen Energy* **40**, 1651 (2015).
- [14] X. Duan, Y. Li, and C. Gao, Constraining the lattice fluid dark energy from SNe, Ia, BAO and OHD, *Sci. China Phys. Mech. Astron.* **56**, 1220 (2013).
- [15] M. M. Hasan, Y. G. Li, G. Li, C. B. Park, and P. Chen, Determination of solubilities of CO₂ in linear and branched polypropylene using a magnetic suspension balance and a PVT apparatus, *J. Chem. Eng. Data* **55**, 4885 (2010).
- [16] G. Li, H. Li, J. Wang, and C. B. Park, Investigating the solubility of CO₂ in polypropylene using various EOS models, *Cell. Polym.* **25**, 237 (2006).
- [17] Y. G. Li, C. B. Park, H. B. Li, and J. Wang, Measurement of the PVT property of PP/CO₂ solution, *Fluid Phase Equilib.* **270**, 15 (2008).
- [18] Y. G. Li and C. B. Park, Effects of branching on the pressure-volume-temperature behaviors of PP/CO₂ solutions, *Ind. Eng. Chem. Res.* **48**, 6633 (2009).
- [19] S. Costeux, CO₂-blown nanocellular foams, *J. Appl. Polym. Sci.* **131**, 41293 (2014).
- [20] S. H. Mahmood, C. L. Xin, J. H. Lee, and C. B. Park, Study of volume swelling and interfacial tension of the polystyrene-carbon dioxide-dimethyl ether system, *J. Colloid Interface Sci.* **456**, 174 (2015).
- [21] M. A. Bashir, M. Al-haj Ali, V. Kanellopoulos, J. Seppälä, E. Kokko, and S. Vijay, The effect of pure component characteristic parameters on Sanchez-Lacombe equation-of-state predictive capabilities, *Macromol. React. Eng.* **7**, 193 (2013).
- [22] I. C. Sanchez and P. A. Rodgers, Solubility of gases in polymers, *Pure Appl. Chem.* **62**, 2107 (1990).
- [23] S. H. Mahmood, M. Keshtkar, and C. B. Park, Determination of carbon dioxide solubility in polylactide acid with accurate PVT properties, *J. Chem. Thermodyn.* **70**, 13 (2014).
- [24] C. G. Panayiotou, Thermodynamics of gas solubility in polymeric liquids, *Makromol. Chem.* **187**, 2867 (1986).
- [25] E. Neau, A consistent method for phase equilibrium calculation using the Sanchez-Lacombe lattice-fluid equation of state, *Fluid Phase Equilib.* **203**, 133 (2002).
- [26] K. von Konigslow, C. B. Park, and R. B. Thompson, Evaluating characteristic parameters for carbon dioxide in the Sanchez-Lacombe equation of state, *J. Chem. Eng. Data* **62**, 585 (2017).
- [27] C. Nicolas, E. Neau, S. Meradji, and I. Raspo, The Sanchez-Lacombe lattice fluid model for the modeling of solids in supercritical fluids, *Fluid Phase Equilib.* **232**, 219 (2005).
- [28] M. W. Matsen, The standard Gaussian model for block copolymer melts, *J. Phys. Condens. Matter* **14**, R21 (2002).
- [29] R. B. Thompson, C. B. Park, and P. Chen, Reduction of polymer surface tension by crystallized polymer nanoparticles, *J. Chem. Phys.* **133**, 144913 (2010).
- [30] G. H. Fredrickson, V. Ganesan, and F. Drolet, Field-theoretic computer simulation methods for polymers and complex fluids, *Macromolecules* **35**, 16 (2002).
- [31] C. I. Poser and I. C. Sanchez, Interfacial tension theory of low and high molecular weight liquid mixtures, *Macromolecules* **14**, 361 (1981).
- [32] D. W. Marquardt, An algorithm for least-squares estimation of nonlinear parameters, *J. Soc. Ind. Appl. Math.* **11**, 431 (1963).
- [33] S. J. Ahn, *Lecture Notes in Computer Science*, Vol. 1070 (Springer, Berlin, 2004).
- [34] G. Li, J. Wang, C. B. Park, and R. Simha, Measurement of gas solubility in linear/branched PP melts, *J. Polym. Sci., Part B: Polym. Phys.* **45**, 2497 (2007).
- [35] Y. G. Li, Ph.D. thesis, University of Toronto, 2008.